Research Article

EASL EUROPEAN ASSOCIATION FOR THE STUDY OF THE LIVER | JOURNAL OF HEPATOLOGY

Intravenous administration of multipotent stromal cells prevents the onset of non-alcoholic steatohepatitis in obese mice with metabolic syndrome

Marcelo Ezquer, Fernando Ezquer, Micaela Ricca, Carolina Allers, Paulette Conget*

Instituto de Ciencias, Facultad de Medicina Clinica Alemana Universidad del Desarrollo, Santiago, Chile

Background & Aims: Metabolic syndrome is secondary to obesity and characterized by dyslipidemia, insulin resistance, and hypertension. Non-alcoholic fatty liver disease is its hepatic manifestation, whose progression-limiting step is non-alcoholic steatohepatitis (NASH). The latter is characterized by lipid accumulation, hepatocyte damage, leukocyte infiltration, and fibrosis. NASH is a prodrome to cirrhosis and hepatocellular carcinoma. Multipotent stromal cells (MSCs) have been shown to be immunomodulatory and contribute to liver regeneration in acute failure conditions.

Our aim was to evaluate whether MSC administration prevents the onset of NASH in obese mice with metabolic syndrome.

Methods: C57BL/6 mice were chronically fed with high-fat diet. At week 33, mice received intravenously either the vehicle (obese untreated) or two doses of 0.5×10^6 syngeneic MSCs (obese MSC-treated). Four months later, liver function and structure, and metabolic syndrome markers were assessed. The persistence of donor $MSCs^{GFP}$ in obese mice was evaluated 17 weeks after their administration.

Results: Obese untreated mice presented high plasma levels of hepatic enzyme, hepatomegaly, liver fibrosis, inflammatory cell infiltration, and hepatic triglyceride accumulation. Furthermore, they showed high expression levels of fibrosis markers and pro-inflammatory cytokines. By contrast, obese MSC-treated mice only presented steatosis. Mice kept obese, hypercholesterolemic, hyperglycemic, and insulin resistant irrespective of whether they received MSCs or not. Donor $MSCs^{GFP}$ were found in liver, bone marrow, heart, and kidney of obese mice.

Conclusions: MSC administration prevents the onset of NASH in obese mice. Observed hepatoprotection is not related to a reversion of the metabolic syndrome but to the preclusion of the inflammatory process.

Keywords: Obesity; Metabolic syndrome; Non-alcoholic fatty liver disease; Non-alcoholic steatohepatitis; Multipotent stromal cells; Mesenchymal stem cells; Hepatoprotection; Prevention.

Received 21 April 2010; received in revised form 22 January 2011; accepted 11 February 2011; available online 26 February 2011

* Corresponding author. Address: Av. Las Condes 12,438, Lo Barnechea, Santiago 7710162, Chile. Tel.: +56 2 327 9157; fax: +56 2 299 9306.

E-mail address: pconget@udd.cl (P. Conget).

Abbreviations: NAFLD, non-alcoholic fatty liver disease; NASH, non-alcoholic steatohepatitis; MSC, multipotent stromal cell, mesenchymal stem cell; HFD, high fat diet.

Introduction

Changes in lifestyle, mainly hypercaloric diet ingestion and sedentarism, result in a dramatic increase in the incidence of the metabolic syndrome, a cluster of clinical features linked to visceral obesity and characterized by dyslipidemia, insulin resistance, and hypertension [1]. Its hepatic manifestation is known as non-alcoholic fatty liver disease (NAFLD) [2]. According to morphological and functional alterations, three stages of NAFLD have been described [3]. First, steatosis that corresponds to lipid accumulation; second, non-alcoholic steatohepatitis (NASH) characterized by steatosis, hepatocyte damage, leukocyte infiltration, and fibrosis; and third, cirrhosis due to scarring accompanied by a rearrangement of organ circulation and a major impairment of liver function [4,5]. A two-hit theory has been proposed to explain NAFLD progression [6]. The first hit depends on insulin resistance. Liver free fatty acids augment and are esterified to triglycerides that accumulate into the hepatocytes, increasing their susceptibility to damage. The second hit relates to oxidative stress and pro-inflammatory environment. It results in the death of hepatocytes, and leads to Kupffer cell activation and hepatic inflammation. Infiltrating leukocytes produce fibrogenic factors, which stimulate hepatic stellate cells to overproduce collagen type I, resulting in fibrosis and further cirrhosis [3,7]. NASH is a critical turning point in NAFLD progression and associates with cirrhosis and hepatocellular carcinoma development [8,9].

To treat patients with NAFLD there is an algorithm that includes body weight control and physical exercise [10], however, it is useful only for some individuals. On the other hand, pharmacological treatments targeted to improve insulin resistance or antioxidant defenses are modestly effective. Therefore, nowadays medical interventions focus on the management of risk factors, early detection of patients who progress to cirrhosis, and liver transplantation in patients with end-stage disease [11,12]. The growing list of patients needing a transplant, the exclusion of several patients as recipient due to the presence of comorbid factors, and the limited availability of organ donors, make chronic liver diseases untreatable for most of the patients [13].

Recently, stem cells have been envisioned as a promising tool for the development of therapeutic strategies to treat patients with

liver diseases [14,15]. Among the different types of bone marrow-derived stem cells, multipotent stromal cells (MSCs) also referred to as mesenchymal stem cells seem to be excellent candidates since they: (i) can be easily isolated from bone marrow aspirates, and efficiently *ex vivo* expanded [16]; (ii) do not require host conditioning before their administration, as in the case of transplantation of whole bone marrow or hematopoietic stem cells [17]; (iii) home into acute damaged liver when systemically administered [18]; (iv) have the ability to manage oxidative stress [19]; (v) are hypoimmunogenic and immunomodulatory, so besides not being recognized by the recipient's immune system when allogeneic transplanted, they could manage exacerbated inflammatory process [17,20]; (vi) can be differentiated, among other cells, into hepatocytes [21]; (vii) produce trophic factors that prevent the apoptosis of parenchymal cells, and induce the proliferation and differentiation of endogenous progenitors [22,23].

Here, our aim was to evaluate whether the intravenous administration of MSCs prevents the onset of NASH. For this, obesity was induced in C57BL/6 mice by chronic feeding with a standardized high-fat diet (HFD). Under this condition, animals develop metabolic syndrome and NAFLD [24,25]. Thirty-three weeks after obesity induction, mice were distributed into two experimental groups matched for average body weight (Fig. 1). One group received the vehicle (obese untreated) and the other group received intravenously two doses, with an elapse of one month, of 0.5×10^6 syngeneic MSCs each (obese MSC-treated). Obese untreated and obese MSC-treated mice continued eating HFD up to 50 weeks. A third group of animals were fed with regular diet all along the study period (normal). Body weight of each animal was monitored twice a week. Before and 17 weeks after MSC administration (weeks 33 and 50 after obesity induction), liver blood chemistry (albumin, total bilirubin, lactate dehydrogenase, alkaline phosphatase, alanine aminotransferase, and aspartate aminotransferase), liver mass, liver histology (fibrosis, inflammation, fatty infiltration), liver gene expression of fibrosis markers, pro-inflammatory cytokines and lipid metabolism genes, and liver lipid (total lipids, triglycerides, cholesterol) content were determined. Also, triglyceridemia, cholesterolemia, glycemia, insulinemia, and glucose tolerance were assessed. In addition, persistence of donor cells was evaluated 17 weeks after the intravenous administration of the first of two doses of 0.5×10^6 MSCs isolated from C57BL/6-Tg ACTB-EGFP 1Osb mice that constitutively express GFP (MSCs^{GFP}), into normal or obese (33 weeks after obesity induction) C57BL/6 mice.

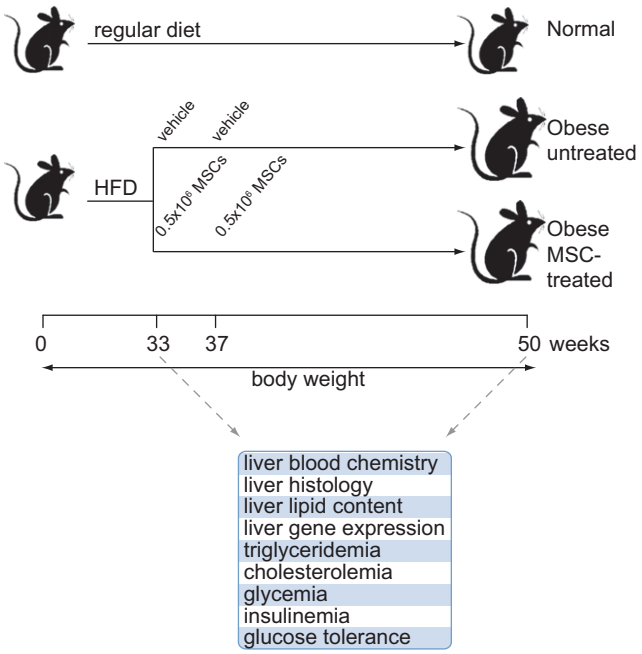

Fig. 1. Experimental design. After 33 weeks of HFD feeding, male C57BL/6 mice were separated into two groups matched for average body weight. One group received two doses of 0.5×10^6 MSCs (obese MSCs-treated). The other group received the vehicle (obese untreated). Both groups were fed HFD during all study period (50 weeks). A third group of mice was fed exclusively with regular diet (normal). During the follow up period, body weight was determined twice a week. At weeks 33 and 50, listed parameters were evaluated.

Materials and methods

Animals

Male C57BL/6 and C57BL/6-Tg ACTB-EGFP 1Osb mice were housed at constant temperature (22 ± 2 °C) and 60% relative humidity, with a 12:12 light–dark cycle. Mice had *ad libitum* access to food and autoclaved water. When required, animals were lightly anesthetized with sevofluorane (Abbott, Japan) or sacrificed by intracardiac injection of thiopental after being anesthetized by intramuscular injection of xylazine and ketamine. All animal protocols used were approved by the Ethics Committee of Facultad de Medicina Clinica Alemana-Universidad del Desarrollo.

Diets

Regular diet: 10 cal% fat, 20 cal% proteins, and 70 cal% carbohydrates (Champion, Chile).
HFD: 60 cal% fat (lard), 20 cal% proteins, and 20 cal% carbohydrates (D12492) (Research Diets Inc., NJ, USA).

Obesity induction

Up to five week-old mice were fed with regular diet. Then, mice were switched to HFD and maintained under this diet for 50 weeks.

Blood triglycerides, cholesterol, glucose, and insulin determination

After 4 h of fasting, mice were sacrificed and blood samples were collected. Serum triglycerides and cholesterol levels were determined in the Abbott Architect c8000 autoanalyzer. Blood glucose levels were measured with the glucometer system Accu-Chek Go (Roche Diagnostic, Germany). Plasma insulin levels were assayed using a mouse-specific insulin ELISA kit (Ultrasensitive Mouse Insulin ELISA; Mercodia, Sweden).

Glucose tolerance test

After 6 h of fasting, mice were lightly anesthetized and injected intraperitoneally with 2 mg glucose/g body weight. Blood glucose levels were determined 15 min before and 15, 30, 60, 90, 120, and 180 min after glucose administration. Area under the curve was determined by the trapezoidal rule.

Liver blood chemistry

After 4 h of fasting, mice were sacrificed and blood samples were collected. Serum albumin, total bilirubin, lactate dehydrogenase, alkaline phosphatase, alanine aminotransferase, and aspartate aminotransferase levels were determined in the Abbott Architect c8000 autoanalyzer.

Liver histology

Liver samples were fixed overnight in 4% paraformaldehyde in phosphate buffer saline (PBS) at 4 °C. Serial 3 μm sections of the right lobes of the liver were stained with hematoxylin and eosin (H&E) and Masson's trichrome. Frozen sections were stained with Oil Red O. Images were captured with a digital camera and analyzed blindly by two observers.

Liver lipid determination

Liver samples were homogenized and lipids were extracted by the method described by Bligh and Dyer [26], with slight modifications. Briefly, 100 mg of tissue were homogenized in 0.5 ml PBS, and the homogenate was added to 5 ml of methanol–chloroform (1:2 V/V). The mixture was extracted overnight at 4 °C and centrifuged at 2000*g* for 10 min. The lower chloroform phase was withdrawn, and lipids in this phase were dried with a stream of nitrogen and weighed for total lipids determination. Total lipids were dissolved in 1 ml of hexane and aliquots were used to determine triacylglycerol and cholesterol with assay kits TG color and Colestat, respectively (Wiener Lab., Argentina).

Liver gene expression analysis

Expression levels of *collagen type I*, *TGF-beta1*, *alpha-smooth muscle actin*, *IL-1beta*, *INF-gamma*, *TNF-alpha*, *FAT-CD36*, *SRBEP1a*, *FAS*, *ACO*, *ACC1*, *CYP2E1*, *CYP4A10*, *CYP4A14*, and *GAPDH* in liver samples were assessed by quantitative RT-PCR. For this, total RNA was purified using TRIzol (Invitrogen, CA, USA) and quantify by absorbance at 260 nm. One μg of total RNA was used for reverse transcription. Real time PCR was performed in a final volume of 10 μl containing 50 μg of cDNA, PCR LightCycler-DNA Master SYBRGreen reaction mix (Roche, IN, USA), 3 mM $MgCl_2$, and 0.5 μM of each specific primer (Supplementary Table 1), using a LightCycler thermocycler (Roche). To ensure that amplicons were from mRNA and not from genomic DNA amplification, controls without reverse transcription were included. Amplicon analysis was performed based on its size and melting point (Supplementary Table 1). Relative quantification was performed by the method described by Schmitten *et al.* [27]. The mRNA level of a target gene was normalized against the mRNA level of *GAPDH* and expressed as change *versus* normal mice.

MSC and MSC^{GFP} isolation and ex vivo expansion

Six to eight week-old male C57BL/6 or C57BL/6-Tg ACTB-EGFP 1Osb mice were sacrificed by cervical dislocation. Bone marrow cells were obtained by flushing femurs and tibias with sterile PBS. After centrifugation, cells were resuspended

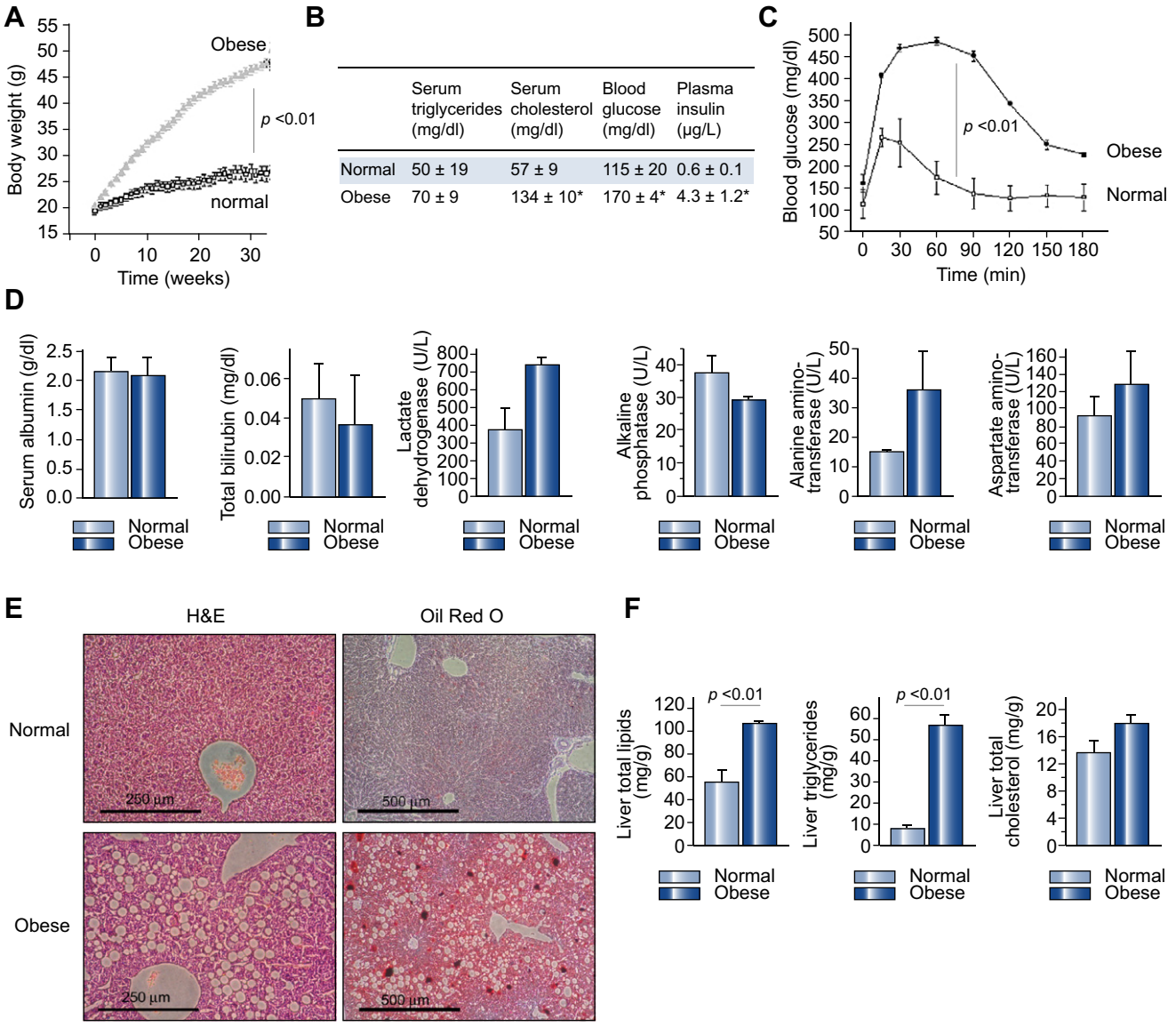

Fig. 2. MSC recipients were obese, with metabolic syndrome, and at first stage of NAFLD. At week 33, compared with mice fed with regular diet (normal), mice fed with HFD (obese) showed (A) high body weight (n = 20), (B) high serum cholesterol, blood glucose, and plasma insulin levels (*p <0.01, n = 6), (C) impaired glucose tolerance test (n = 8), (D) similar liver blood chemistry (n = 4), (E) accumulation of neutral lipids (n = 3), and (F) high triglyceride content in the liver (n = 10).

in alpha-MEM (Gibco, NZ) supplemented with 10% selected fetal bovine serum (Gibco) and 80 mg/ml gentamicin (Sanderson Laboratory, Chile), and plated at a density of 1×10^6 nucleated cells/cm^2. Non-adherent cells were removed after 72 h by media change. When foci reached confluence, adherent cells were detached with 0.25% trypsin, 2.65 mM EDTA (Gibco), centrifuged, and subcultured at 7000 cells/cm^2. After two subcultures, adherent cells were characterized and transplanted.

MSC characterization

Although there are currently no consensus markers for murine MSCs as there exist for human MSCs [28], immunophenotyping was performed by flow cytometry analysis after immunostaining with monoclonal antibodies against putative murine MSC markers SCA-1 (APC-conjugated), CD90 (PE-conjugated), CD44 (PE-Cy5-conjugated) (all from eBioscience, CA, USA), and lymphocyte markers B220, CD4, CD8 (PE-Cy5-conjugated) (all from BD Pharmingen, CA, USA).

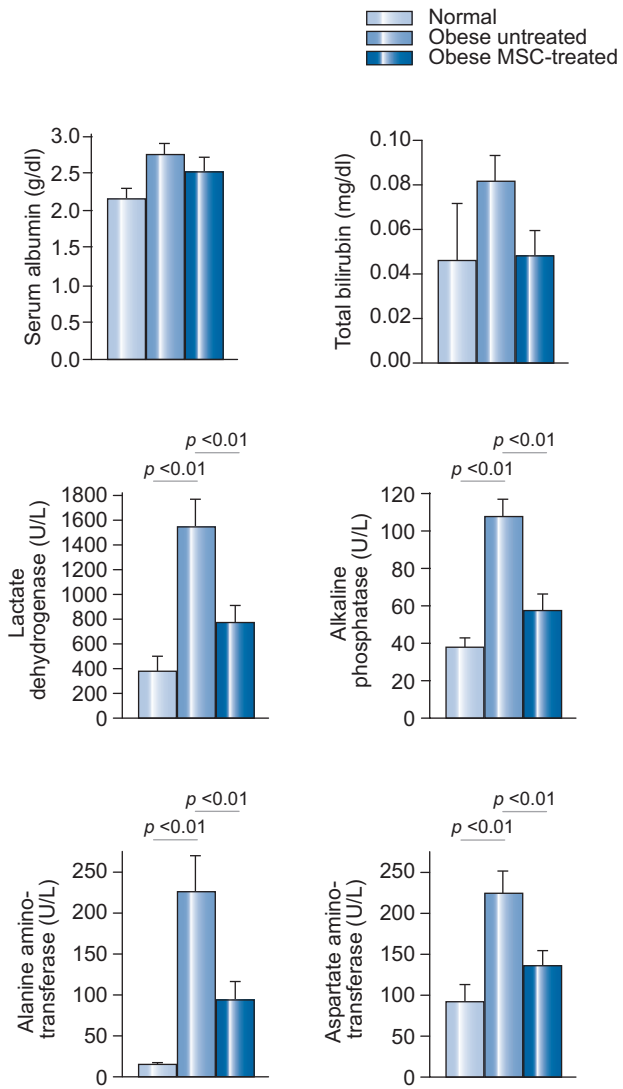

Fig. 3. MSC administration prevents liver injury secondary to obesity-induced metabolic syndrome. At week 50, compared with normal mice, obese untreated mice showed slightly increased levels of hepatocyte functional marker (total bilirubin), high levels of cellular damage markers (lactate dehydrogenase and alkaline phosphatase), and hepatocellular damage markers (alanine aminotransferase and aspartate aminotransferase). Compared with untreated obese mice, MSC-treated mice presented low levels of liver injury markers. Compared with normal mice, MSC-treated mice presented similar levels of assessed markers. Each group n = 8.

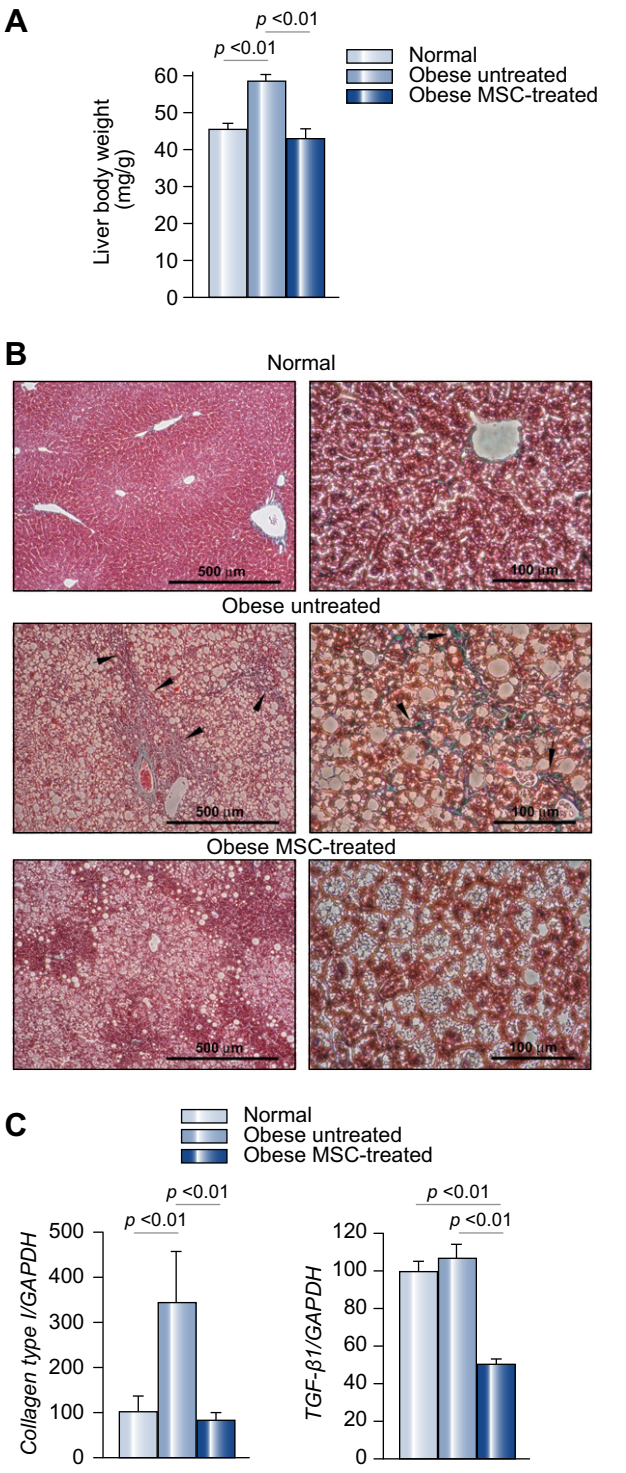

Fig. 4. MSC administration prevents hepatomegaly and liver fibrosis secondary to obesity-induced metabolic syndrome. At week 50, compared with normal mice, obese untreated mice showed (A) high liver/body weight ratio, (B) liver perivenular and pericellular deposition of collagen fibers revealed by Masson's trichrome stain (arrows), and (C) high collagen type I gene expression in the liver. Compared with obese untreated mice, MSC-treated mice showed low liver/body weight ratio, no Masson's trichrome staining, and low mRNA levels of *collagen type I* and *TGF-beta1*. Compared with normal mice, MSC-treated mice showed similar liver size, similar collagen type I expression but low *TGF-beta1* mRNA levels in the liver. Each group n = 8.

MSC proliferation potential was assessed after culturing cells at 4000 cells/cm^2 and determining cell number at days 0, 2, 5, 7, 9, 12, and 15 by staining with 0.5% crystal violet in 10% methanol. After four washes, cell-incorporated crystal violet was solubilized by incubation with phosphate buffer in methanol (50:50) and quantified spectrophotometrically (absorbance at 570 nm). MSC differentiation potential was assessed after cells exposure to standard adipogenic or osteogenic differentiation media for 14 and 21 days, respectively [16].

MSC or MSC^{GFP} intravenous administration

0.5×10^6 MSCs or 0.5×10^6 MSCs^{GFP} were resuspended in 0.2 ml of 5% mice plasma (vehicle) and administered via the tail vein to lightly anesthetized mice. Untreated animals received 0.2 ml of vehicle.

Donor MSC^{GFP} detection in recipient organs

Animals were deeply anesthetized, exsanguinated, and intracardially perfused with washing solution (0.8% NaCl, 0.8% sucrose, and 0.4% glucose) for 10 min. Blood, heart, lung, pancreas, intestine, kidney, liver, spleen, and bone marrow were obtained from normal, obese untreated, and obese MSC^{GFP}-treated mice. For flow cytometry analysis, solid organs were weighted, washed twice with ice-cold PBS, chopped and digested with 1 mg/ml collagenase type II (Gibco) for 30 min at 37 °C. Cell suspension thus obtained was filtered through a 100 μm strainer and washed twice with ice-cold PBS. Isolated cells were fixed, permeabilized with BD Cytofix/Cytoperm kit (BD Bioscience, CA, USA), and resuspended in 1 ml of PBS with 2% fetal bovine serum plus 0.5 μl of undiluted antibody anti-GFP AlexaFluor 647 (Molecular Probes, OR, USA). After 12 h of incubation at 4 °C, cells were washed, filtered through a 30 μm mesh, and acquired in a CyAn ADP flow cytometer (DakoCytomation, CA, USA) [29]. Data were analyzed with Summit v4.3 software and criteria used to consider an event as an MSC^{GFP} were FSC and SSC similar to *ex vivo* expanded MSCs and positive fluorescence, both in FL1 (GFP) and FL8 (anti GFP-AlexaFluor 647) channels. Tissues from normal and obese untreated mice were used as control of autofluorescence. For each organ, acquisition was performed up to detection of 100 events that fulfilled the criteria of an MSC^{GFP}. In the case of organs where donor MSCs^{GFP} were not detectable, a total of 500,000 events were acquired [30].

For *in situ* detection of MSC^{GFP}, after perfusion with washing solution, animals were perfused with 4% paraformaldehyde in 0.01 M borate buffer pH 7.4, containing 0.35 M Na_2SO_3. Livers were dissected and stored in paraformaldehyde at 4 °C overnight. On the following day, they were cryoprotected with 30% sucrose in buffered paraformaldehyde. Two days later, livers were rapidly frozen at −20 °C in isopentane, and serially sectioned (30 μm). Sections were mounted, washed with PBS, stained with rabbit anti-GFP antibody (eBioscience) at 4 °C overnight followed by goat anti-rabbit-FITC conjugated serum (Vector Labs, Burlingame, CA) at room temperature for 1 h and counterstained with Topro-3 (Invitrogen). To determine whether donor cells express albumin, sections were further stained with goat anti-albumin antibody (Novus Biologicals, CO, USA) and donkey anti-goat-Alexa-Fluor 555 conjugated serum (Invitrogen). Samples were examined in a LSM Meta Zeiss confocal microscope and analyzed with the Zeiss LSM Image Bowser software.

Statistical analysis

Data are presented as mean ± S.E.M. To determine the statistical significances of intergroup differences, Kruskal–Wallis test was used to compare mean values among all groups and Mann–Whitney *U* test was used to compare mean values between two groups. $p < 0.05$ was considered as statistically significant.

Results

MSC recipients were obese, with metabolic syndrome, and at the first stage of NAFLD

Mice fed with HFD progressively augmented their body weight (Fig. 2A). At 33 weeks, they almost doubled the body weight of normal mice (46.6 ± 0.9 *vs.* 26.8 ± 1.4 g). Serum cholesterol, blood glucose, and plasma insulin levels were increased in obese mice (Fig. 2B). While normal mice showed a normal glucose tolerance test, obese mice were glucose intolerant (Fig. 2C). Thirty-three weeks after obesity induction, liver blood chemistry was not significantly modified (Fig. 2D), while liver deposition of triglycerides was evidenced histologically (Fig. 2E) and molecularly (Fig. 2F). No liver fibrosis was detected at this time point (data not shown).

MSC administration prevents liver injury secondary to obesity-induced metabolic syndrome

Fifty weeks after obesity induction, untreated mice presented basal levels of serum albumin and high levels of serum total bilirubin, lactate dehydrogenase, alkaline phosphatase, alanine aminotransferase, and aspartate aminotransferase (Fig. 3). In contrast, obese mice receiving MSCs that have been *ex vivo* expanded and characterized according to their immunophenotype, proliferation, and differentiation potentials (Supplementary Fig. 1) presented basal levels of those markers. While lactate dehydrogenase and alkaline phosphatase are liver-unspecific, the aminotransferases are indicative of liver damage. Thus, MSC administration protects liver from injury and preserves its function.

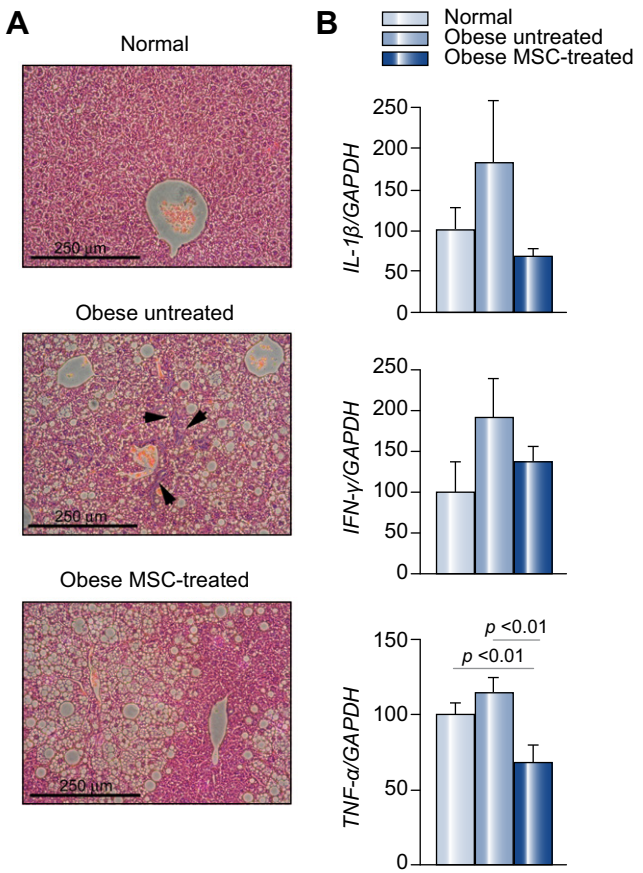

Fig. 5. MSC administration prevents liver inflammation secondary to obesity-induced metabolic syndrome. At week 50, compared to normal mice, the liver of obese untreated mice showed (A) inflammatory infiltrates (arrows) and (B) slightly high *IL-1beta* and *INF-gamma* gene expression. Compared with obese untreated mice, MSC-treated mice showed no inflammatory focus and low levels of all pro-inflammatory cytokines assessed. Compared with normal mice, MSC-treated mice showed low *TNF-alpha* mRNA levels. Each group n = 8.

MSC administration prevents hepatomegaly and liver fibrosis secondary to obesity-induced metabolic syndrome

The liver of obese untreated mice was paler, larger, and heavier than those of normal mice. MSC administration prevents hepatomegaly observed in obese untreated mice (Fig. 4A).

Perisinusoidal and pericellular fibrosis was detected in the liver of obese untreated mice (Fig. 4B), while no fibrosis was observed in obese MSC-treated mice. Accordingly, the expression of collagen type I was three times higher in obese untreated mice than in normal ones, whereas no changes were detected in obese MSC-treated mice (Fig. 4C). The fibrogenic factor TGF-beta1 was significantly reduced in obese MSC-treated mice, as compared to normal and obese untreated mice (Fig. 4C). On the other hand, the expression of alpha-smooth muscle actin was similar in all experimental groups (data not shown).

MSC administration prevents liver inflammation secondary to obesity-induced metabolic syndrome

Multifocal inflammatory cellular foci were evidenced in the liver of obese untreated mice (Fig. 5A). In contrast, no leukocyte infiltration was observed in obese mice treated with MSCs. Accordingly, the levels of *IL-1beta*, *INF-gamma*, *TNF-alpha*, and *TGF-beta1* mRNAs were lower in obese MSC-treated mice than in obese untreated ones (Figs. 4C and 5B).

MSC administration slightly reverts steatosis secondary to obesity-induced metabolic syndrome

Obese mice accumulated neutral lipids in their liver whether they received MSCs or not (Fig. 6A). While steatosis in obese untreated mice was mostly macrovacuolar, in obese MSC-treated mice the microvacuolar type predominated. When compared with normal mice, obese untreated and obese MSC-treated mice presented high levels of liver total lipids and triglycerides, but normal levels of liver cholesterol (Fig. 6B). Nonetheless, MSC administration slightly reduced the accumulation of triglycerides in the liver of obese mice with metabolic syndrome.

The liver expression of sterol regulatory element binding protein 1a (*SREBP1a*), acetyl-CoA carboxilase 1 (*ACC1*), *CYP4A10*, and *CYP4A14* genes was not modified by HFD feeding (Fig. 6C and data not shown, respectively). However, in obese untreated mice the mRNA levels of *FAT-CD36* and fatty acid synthase (*FAS*) were significantly increased (Fig. 6C and data not shown, respectively) and those of acetyl CoA oxidase (*ACO*) and *CYP2E1* were reduced (Fig. 6C). In obese MSC-treated mice, the liver expression of the enzymes involved in fatty acid oxidation was not impaired (Fig. 6C).

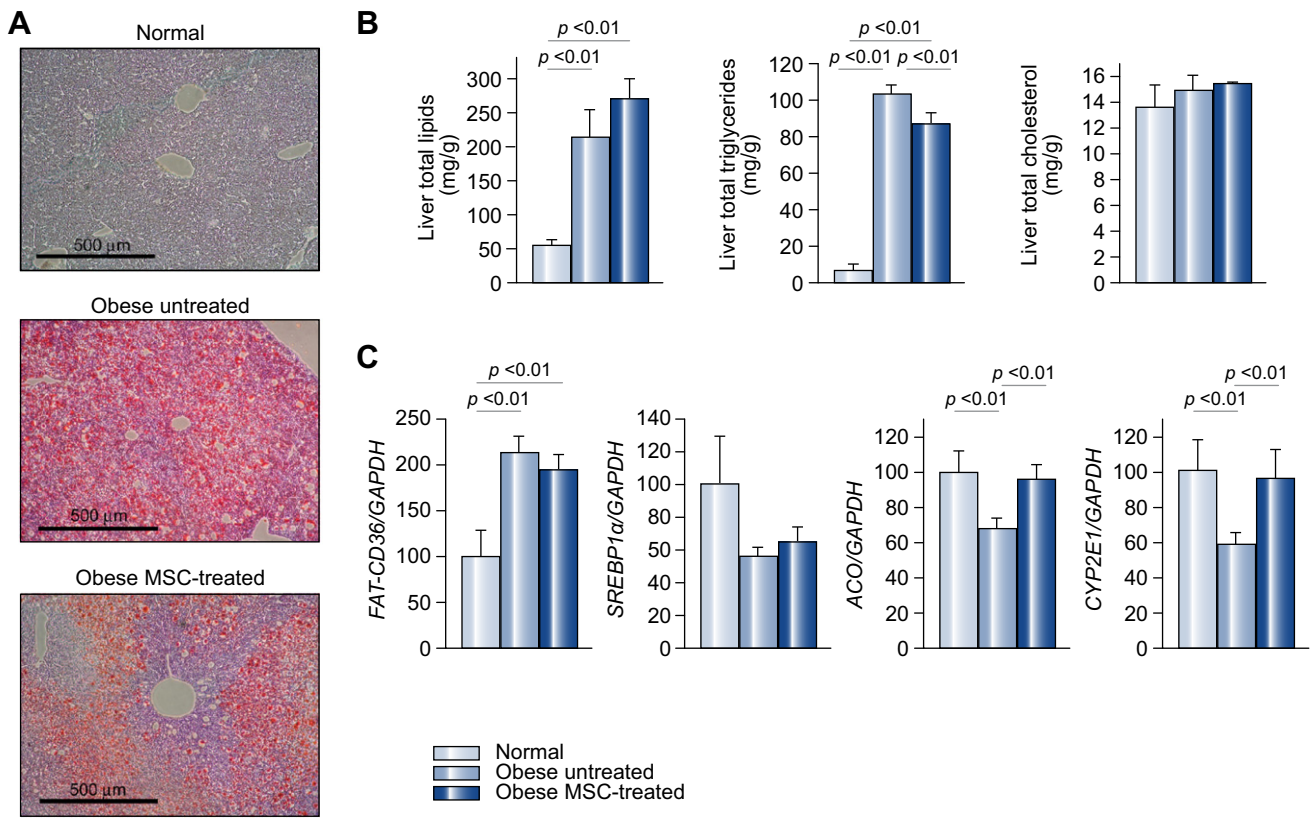

Fig. 6. MSC administration slightly reverts steatosis secondary to obesity-induced metabolic syndrome. At week 50, compared with normal mice, the liver of obese untreated mice showed (A) micro- and macrovacuolization of hepatocytes, revealed after Oil Red O stain, (B) high levels of lipids and triglycerides but not cholesterol, and (C) increased *FAT-CD36* and diminished *SREBP1a*, *ACO*, and *CYP2E1* mRNA levels. Compared with obese untreated mice, MSC-treated mice showed mainly microvacuolar neutral lipid accumulations, low levels of triglycerides, and high levels of *ACO* and *CYP2E1* expression. Compared with normal mice, MSC-treated mice showed steatosis, high levels of lipids and triglycerides, and similar levels of *ACO* and *CYP2E1*. Each group n = 8.

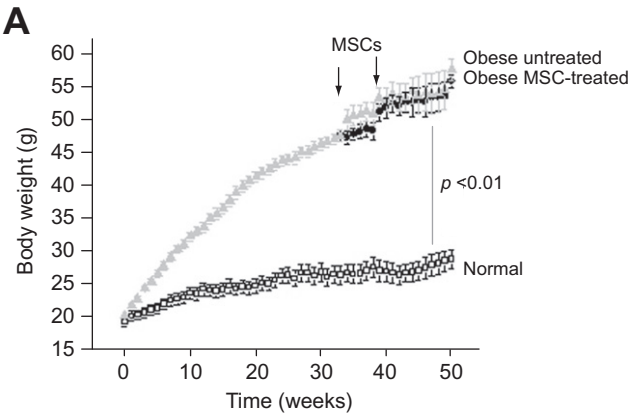

B

	Serum triglycerides (mg/dl)	Serum cholesterol (mg/dl)	Blood glucose (mg/dl)	Plasma insulin (μg/L)
Normal	43 ± 16	57 ± 5	121 ± 7	0.5 ± 0.1
Obese untreated	59 ± 9	202 ± 14*	173 ± 6*	8.6 ± 0.9*
Obese MSC-treated	71 ± 9	184 ± 8*	164 ± 4*	6.8 ± 2*

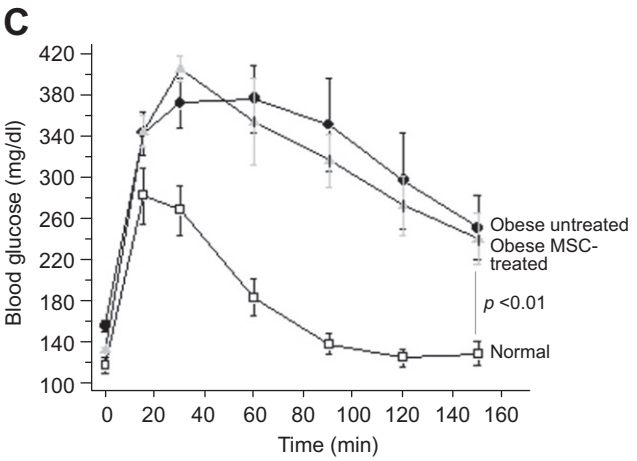

Fig. 7. MSC administration reverts neither metabolic syndrome nor obesity. At week 50, compared with normal mice, obese mice showed (A) high body weight (n = 20), (B) high serum cholesterol, blood glucose, and plasma insulin levels (*p <0.01, n = 10), and (C) impaired glucose tolerance test (n = 8), whether they received or not MSC. At week 33, body weights were: normal = 26.8 ± 1.4 g, obese untreated = 47.7 ± 1.5 g, obese MSC-treated = 46.9 ± 1.1 g. Mean difference between obese untreated and obese MSC-treated = 0.8, p >0.05, 95% CI of difference = 3.82–5.42). At week 37, body weights were: normal = 27.5 ± 1.4 g, obese untreated = 51.4 ± 1.5 g, obese MSC-treated = 48.7 ± 1.2 g. Mean difference between obese untreated and obese MSC-treated = 2.7, p >0.05, 95% CI of difference = 2.02–7.42). At week 50, body weights were: normal = 29.2 ± 1.5 g, obese untreated = 57.7 ± 1.7 g, obese MSC-treated = 55.9 ± 1.0 g. Mean difference between obese untreated and obese MSC-treated = 1.8, p >0.05, 95% CI of difference = 3.07–6.67).

MSC administration reverts neither metabolic syndrome nor obesity

During the follow up period, no statistically significant changes were observed in body weight of mice either treated or not with MSCs (Fig. 7A). Hypercholesterolemia, hyperglycemia, hyperinsulinemia, and glucose intolerance were not reverted by MSC administration (Fig. 7B and C).

Donor MSCs^{GFP} persist in the liver of obese mice

Donor cells were not detectable in all tested organs obtained from normal mice (Fig. 8A). In contrast, 17 weeks after their administration, MSCs^{GFP} were found in liver, bone marrow, heart, and kidney but not in blood, lung, pancreas, intestines, and spleen of obese mice (Fig. 8B). In the liver of obese mice, donor MSCs^{GFP} appeared as single cells or cell clusters, localized in portal areas and did not express albumin (Fig. 8C and D).

Discussion

NASH is not a benign condition [5]. Five to seven years after been diagnosed, 30% of the patients with NASH progress to liver fibrosis. Furthermore, 15–20% of these patients develop cirrhosis and of these patients who develop cirrhosis, 30–45% suffer liver-related mortality [6,31]. In addition, hepatocellular carcinoma is being increasingly recognized as an important complication in the natural history of NASH [32]. Here, we show that bone marrow-derived MSCs, given intravenously, prevent the onset of NASH. We prove this in a validated model of NAFLD established by chronic feeding endogamic C57BL/6J mice with a HFD [33]. Under this condition, animals develop obesity and systemic insulin resistance. Additionally, the transition from simple steatosis to NASH is observed. Hence, this animal model has been recognized as one of the best in reproducing the progression of NAFLD as occurs in humans [34].

The hepatoprotection observed after MSC administration did not relate to reversion of the metabolic syndrome, since obese MSC-treated mice remain obese, hypercholesterolemic, hyperglycemic, hyperinsulinemic, and glucose intolerant. Moreover, only a minor change in steatosis was observed in these animals. Qualitatively, fat deposits in the liver can be classified as micro- or macrosteatosis. Microsteatosis consists of many small fatty inclusions in the cytoplasm of hepatocytes without displacement of organelles. In contrast, in macrosteatosis, hepatocytes contain one single vacuole of fat that displaces the nucleus to the periphery of the cell. Obese mice that received MSCs did not shift to predominant macrosteatosis as observed in obese untreated animals. Along with, the expression of the enzymes that mediate fatty acid oxidation was not impaired in obese MSC-treated mice as occurs in obese untreated animals. Although the nature of the shift from micro- to macrosteatosis is unknown, it has been suggested that it relates to an impairment of fatty acid catabolism [35], and it has been associated with the progression of NAFLD to an impairment of hepatic function [36]. Accordingly, while serum transaminases increased in obese untreated mice, they remained at normal levels in obese MSC-treated animals. The same was true for cell death markers: lactate dehydrogenase and alkaline phosphatase. In obese MSC-treated mice the histological analysis of hepatic tissue revealed neither signs of fibrosis nor leukocyte infiltration. Intrahepatic gene expression levels of pro-inflammatory cytokines and fibrosis marker (*IL-1beta*, *INF-gamma*, *TNF-alpha*, *TGF-beta1* and *collagen type I*) were equal or even lower in obese MSC-treated mice than in normal mice. The case of TNF-alpha is remarkable because it has been shown that modulation of its expression results in an improvement of NASH [37].

To determine whether the prevention of NASH onset observed after MSC intravenous administration relates to recruitment and permanence of donor cells into the liver of the recipient, we administered MSCs^{GFP} into obese mice with metabolic syndrome.

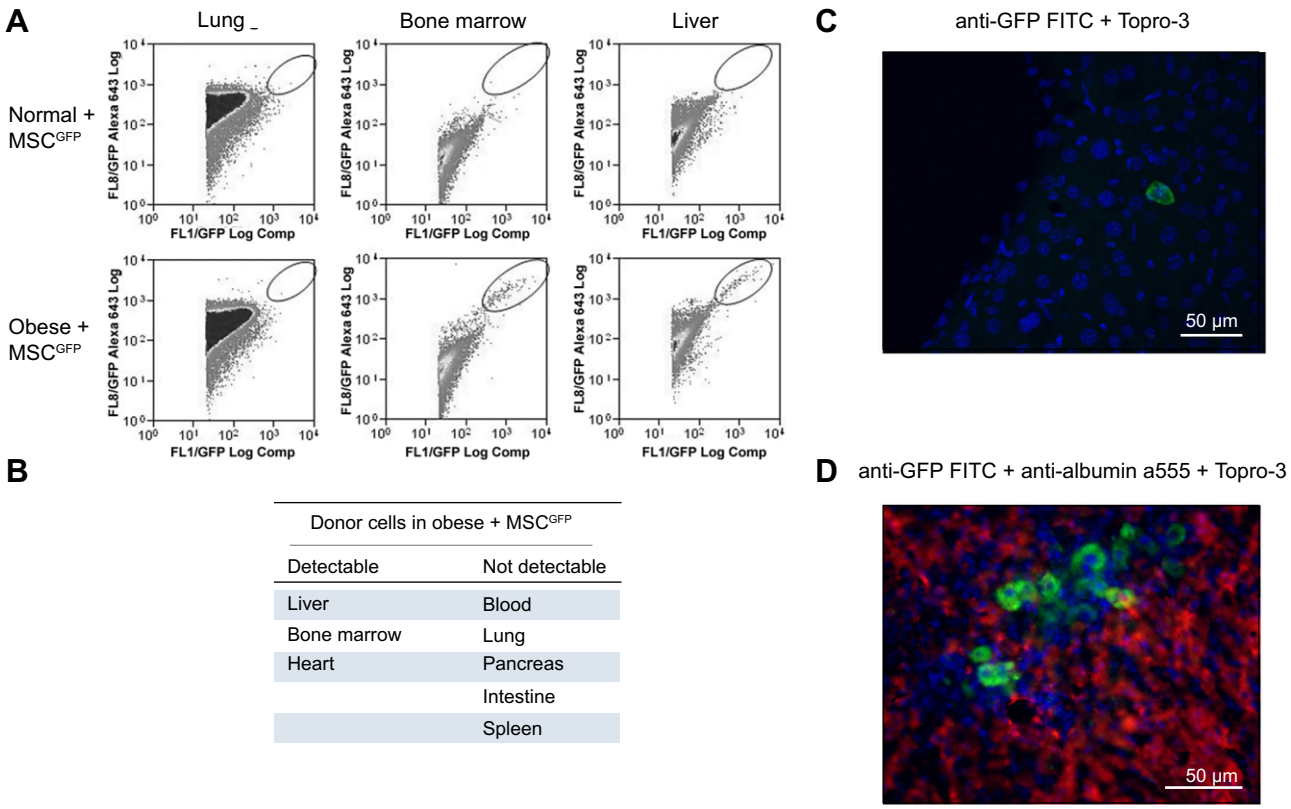

Donor cells in obese + MSC^{GFP}	
Detectable	Not detectable
Liver	Blood
Bone marrow	Lung
Heart	Pancreas
	Intestine
	Spleen

Fig. 8. Donor MSCs^{GFP} persist in the liver of obese mice. After 33 weeks of feeding with regular diet (normal) or HFD (obese), mice received a dose of 0.5×10^6 MSCs^{GFP}. A month later, mice received a second dose of 0.5×10^6 MSCs^{GFP}. Seventeen weeks after the first dose, (A) donor cells were evidenced by flow cytometry in obese mice, but not in normal mice. (B) In obese mice, MSCs^{GFP} were found in the liver, bone marrow, heart and kidney, but not in any other tested organs. In the liver of obese mice, donor MSCs^{GFP} (C) were found around the portal vein and (D) did not express albumin. Each group n = 5.

Seventeen weeks later, donor MSCs^{GFP} were detected in the liver and also in bone marrow, heart, and kidney of obese mice. The selectivity of this recruitment was supported by the fact that no donor cells were detected when MSCs^{GFP} were administered into normal mice. Thus, in agreement with already published data, MSC recruitment to the liver depends on the presence of hepatic injury [18,38]. On the other hand, the fact that donor cells were located around the portal areas is not unexpected, since in other models of tissue injury they were found near the vasculature [39].

Although donor derived cells were detected in the liver of recipients, their scarcity and failure to express albumin suggest that MSC therapeutic effects involve mechanisms other than functional complementation from direct differentiation to parenchymal cells [40]. The role of trophic factors secreted by MSCs has been strongly supported by a recent study reporting a beneficial effect of the administration of MSC-derived biomolecules in acute liver injury [41]. On the other hand, donor MSCs could contribute to limiting acute liver damage induced by oxidative stress [18,19]. Thus, as demonstrated for lung and kidney injuries, local down-regulation of pro-inflammatory cytokines must be related to tissue protection [39,41]. Furthermore, the preclusion of leukocyte infiltration observed in obese MSC-treated mice can explain the prevention of fibrosis development because it has been already demonstrated that infiltrating macrophages and lymphocytes play a pivotal role in the fibrogenic process [36,42,43]. The role of MSCs in liver fibrosis is a matter of controversy. While some studies show a reduction [20,44,45], others show an increase [46], and others show no effect [47]. Here, we show the prevention of liver fibrosis after MSC administration.

Our pre-clinical results demonstrate that the intravenous administration of MSCs prevents the transition from single steatosis to NASH in obese mice with metabolic syndrome. The observed modification of NAFLD progression seems to be related, at least, to pleiotropic local effect of donor MSCs that delay or preclude the appearance of the second hit. To elucidate the molecular mechanism involved here, further investigation is needed.

Conflict of interest

The authors who have taken part in this study do not have a relationship with the manufacturers of the drugs involved either in the past or present and did not receive funding from the manufacterers to carry out their research. The authors received support from the Facultad de Medicina Clinica Alemana – Universidad del Desarrollo.

Acknowledgments

This work was supported by FONDECYT Grants #11085034 to M.E. and PBCT PSD-34 to P.C. We thank Mrs. Valeska Simons for helping us with the flow cytometry analysis and Mrs. Carolina Larrain for English editing of the manuscript.

Supplementary data

Supplementary data associated with this article can be found, in the online version, at doi:10.1016/j.jhep.2011.02.020.

References

[1] Marchesini G, Marzocchi R. Metabolic syndrome and NASH. Clin Liver Dis 2007;11:105–117.
[2] Schwimmer JB, Deutsch R, Rauch JB, Behling C, Newbury R, Lavine JE. Obesity, insulin resistance, and other clinicopathological correlates of pediatric nonalcoholic fatty liver disease. J Pediatr 2003;143:500–505.
[3] Marra F, Gastaldelli A, Svegliati BG, Tell G, Tiribelli C. Molecular basis and mechanisms of progression of non-alcoholic steatohepatitis. Trends Mol Med 2008;14:72–81.
[4] Farrell GC, Larter CZ. Nonalcoholic fatty liver disease: from steatosis to cirrhosis. Hepatology 2006;43:S99–S112.
[5] Harrison SA, Torgerson S, Hayashi PH. The natural history of nonalcoholic fatty liver disease: a clinical histopathological study. Am J Gastroenterol 2003;98:2042–2047.
[6] Lewis JR, Mohanty SR. Nonalcoholic fatty liver disease: a review and update. Dig Dis Sci 2010;55:560–578.
[7] Bataller R, Brenner DA. Liver fibrosis. J Clin Invest 2005;115:209–218.
[8] Caldwell SH, Crespo DM. The spectrum expanded: cryptogenic cirrhosis and the natural history of non-alcoholic fatty liver disease. J Hepatol 2004;40:578–584.
[9] Shimada M, Hashimoto E, Taniai M, Hasegawa K, Okuda H, Hayashi N, et al. Hepatocellular carcinoma in patients with non-alcoholic steatohepatitis. J Hepatol 2002;37:154–160.
[10] Schuppan D, Gorrell MD, Klein T, Mark M, Afdhal NH. The challenge of developing novel pharmacological therapies for non-alcoholic steatohepatitis. Liver Int 2010;30:795–808.
[11] Angulo P. GI epidemiology: nonalcoholic fatty liver disease. Aliment Pharmacol Ther 2007;25:883–889.
[12] Angulo P. Nonalcoholic fatty liver disease and liver transplantation. Liver transpl 2006;12:523–534.
[13] Sass DA, Shakil AO. Fulminant hepatic failure. Liver Transpl 2005;11:594–605.
[14] Kallis YN, Alison MR, Forbes SJ. Bone marrow stem cells and liver disease. Gut 2007;56:716–724.
[15] Sharma AD, Cantz T, Manns MP, Ott M. The role of stem cells in physiology, pathophysiology, and therapy of the liver. Stem Cell Rev 2006;2:51–58.
[16] Conget PA, Minguell JJ. Phenotypical and functional properties of human bone marrow mesenchymal progenitor cells. J Cell Physiol 1999;181:67–73.
[17] Rasmusson I. Immune modulation by mesenchymal stem cells. Exp Cell Res 2006;312:2169–2179.
[18] Kuo TK, Hung SP, Chuang CH, Chen CT, Shih YR, Fang SC, et al. Stem cell therapy for liver disease: parameters governing the success of using bone marrow mesenchymal stem cells. Gastroenterology 2008;134:2111–2121.
[19] Valle-Prieto A, Conget PA. Human mesenchymal stem cells efficiently manage oxidative stress. Stem Cells Dev 2010;19:1885–1893.
[20] Parekkadan B, van PD, Megeed Z, Kobayashi N, Tilles AW, Berthiaume F, et al. Immunomodulation of activated hepatic stellate cells by mesenchymal stem cells. Biochem Biophys Res Commun 2007;363:247–252.
[21] Sato Y, Araki H, Kato J, Nakamura K, Kawano Y, Kobune M, et al. Human mesenchymal stem cells xenografted directly to rat liver are differentiated into human hepatocytes without fusion. Blood 2005;106:756–763.
[22] Caplan AI, Dennis JE. Mesenchymal stem cells as trophic mediators. J Cell Biochem 2006;98:1076–1084.
[23] Phinney DG, Prockop DJ. Concise review: mesenchymal stem/multipotent stromal cells: the state of transdifferentiation and modes of tissue repair – current views. Stem Cells 2007;25:2896–2902.
[24] Gallou-Kabani C, Vige A, Gross MS, Rabes JP, Boileau C, Larue-Achagiotis C, et al. C57BL/6J and A/J mice fed a high-fat diet delineate components of metabolic syndrome. Obesity (Silver Spring) 2007;15:1996–2005.
[25] Ito M, Suzuki J, Tsujioka S, Sasaki M, Gomori A, Shirakura T, et al. Longitudinal analysis of murine steatohepatitis model induced by chronic exposure to high-fat diet. Hepatol Res 2007;37:50–57.
[26] Bligh EG, Dyer WJ. A rapid method of total lipid extraction and purification. Can J Biochem Physiol 1959;37:911–917.
[27] Schmittgen TD, Livak KJ. Analyzing real-time PCR data by the comparative C(T) method. Nat Protoc 2008;3:1101–1108.
[28] Dominici M, Le BK, Mueller I, Slaper-Cortenbach I, Marini F, Krause D, et al. Minimal criteria for defining multipotent mesenchymal stromal cells. The International Society for Cellular Therapy position statement. Cytotherapy 2006;8:315–317.
[29] Allers K, Kunkel D, Moos V, Eisenblatter M, Stahl-Hennig C, Kaup FJ, et al. Migration patterns of nonspecifically activated versus nonactivated nonhuman primate T lymphocytes: preferential homing of activated autologous $CD8^+$ T cells in the rectal mucosa. J Immunother 2008;31:334–344.
[30] Ezquer F, Ezquer M, Simon V, Pardo F, Yanez A, Carpio D, et al. Endovenous administration of bone-marrow-derived multipotent mesenchymal stromal cells prevents renal failure in diabetic mice. Biol Blood Marrow Transplant 2009;15:1354–1365.
[31] Edmison J, McCullough AJ. Pathogenesis of non-alcoholic steatohepatitis: human data. Clin Liver Dis 2007;11:75–104.
[32] Starley BQ, Calcagno CJ, Harrison SA. Nonalcoholic fatty liver disease and hepatocellular carcinoma: a weighty connection. Hepatology 2010;51:1820–1832.
[33] Ito T, Suzuki A, Imai E, Okabe M, Hori M. Bone marrow is a reservoir of repopulating mesangial cells during glomerular remodeling. J Am Soc Nephrol 2001;12:2625–2635.
[34] London RM, George J. Pathogenesis of NASH: animal models. Clin Liver Dis 2007;11:55–74.
[35] El-Badry AM, Graf R, Clavien PA. Omega 3–Omega 6: what is right for the liver? J Hepatol 2007;47:718–725.
[36] Selzner N, Selzner M, Jochum W, mann-Vesti B, Graf R, Clavien PA. Mouse livers with macrosteatosis are more susceptible to normothermic ischemic injury than those with microsteatosis. J Hepatol 2006;44:694–701.
[37] Li Z, Yang S, Lin H, Huang J, Watkins PA, Moser AB, et al. Probiotics and antibodies to TNF inhibit inflammatory activity and improve nonalcoholic fatty liver disease. Hepatology 2003;37:343–350.
[38] Allers C, Sierralta WD, Neubauer S, Rivera F, Minguell JJ, Conget PA. Dynamic of distribution of human bone marrow-derived mesenchymal stem cells after transplantation into adult unconditioned mice. Transplantation 2004;78:503–508.
[39] Caplan AI. Why are MSCs therapeutic? New data: new insight. J Pathol 2009;217:318–324.
[40] Togel F, Hu Z, Weiss K, Isaac J, Lange C, Westenfelder C. Administered mesenchymal stem cells protect against ischemic acute renal failure through differentiation-independent mechanisms. Am J Physiol Renal Physiol 2005;289:F31–F42.
[41] van PD, Parekkadan B, Cho CH, Berthiaume F, Nahmias Y, Tilles AW, et al. Mesenchymal stem cell-derived molecules directly modulate hepatocellular death and regeneration in vitro and in vivo. Hepatology 2008;47:1634–1643.
[42] Wallace K, Burt AD, Wright MC. Liver fibrosis. Biochem J 2008;411:1–18.
[43] Diehl AM, Li ZP, Lin HZ, Yang SQ. Cytokines and the pathogenesis of non-alcoholic steatohepatitis. Gut 2005;54:303–306.
[44] bdel Aziz MT, Atta HM, Mahfouz S, Fouad HH, Roshdy NK, Ahmed HH, et al. Therapeutic potential of bone marrow-derived mesenchymal stem cells on experimental liver fibrosis. Clin Biochem 2007;40:893–899.
[45] Higashiyama R, Inagaki Y, Hong YY, Kushida M, Nakao S, Niioka M, et al. Bone marrow-derived cells express matrix metalloproteinases and contribute to regression of liver fibrosis in mice. Hepatology 2007;45:213–222.
[46] di Bonzo LV, Ferrero I, Cravanzola C, Mareschi K, Rustichell D, Novo E, et al. Human mesenchymal stem cells as a two-edged sword in hepatic regenerative medicine: engraftment and hepatocyte differentiation versus profibrogenic potential. Gut 2008;57:223–231.
[47] Carvalho AB, Quintanilha LF, Dias JV, Paredes BD, Mannheimer EG, Carvalho FG, et al. Bone marrow multipotent mesenchymal stromal cells do not reduce fibrosis or improve function in a rat model of severe chronic liver injury. Stem Cells 2008.